

*Article***Cavity-Assisted Spin-Orbit Coupling of Ultracold atoms****Lin Dong**<sup>1</sup>, **Chuanzhou Zhu**<sup>1</sup> and **Han Pu**<sup>1\*</sup><sup>1</sup> Department of Physics and Astronomy, Rice Quantum Institute, Rice University, Houston, Texas, 77251-1892, USA

\* Author to whom correspondence should be addressed; hpu@rice.edu

*Version March 3, 2015 submitted to Atoms. Typeset by L<sup>A</sup>T<sub>E</sub>X using class file mdpi.cls*


---

**Abstract:** We investigate dynamical and static properties of ultracold atoms confined in an optical cavity, where two photon Raman process induces effective coupling between atom's pseudo-spin and center-of-mass momentum. In the meantime, atomic dynamics exerts a back action to cavity photons. We adopt both mean field and master equation approach to tackle the problem and found surprising modifications to atomic dispersions and dynamical instabilities, arising from the intrinsic nonlinearity of the system. Correspondence between semi-classical and quantum limits is analyzed as well.

**Keywords:** cavity quantum electrodynamics; cold atoms; spin-orbit coupling

---

**1. Introduction**

When Jaynes and Cummings first studied the time evolution of a two-level atom in an electromagnetic field in a *fully* quantized way in 1960s [1], experimental realization of this ideal theoretical model was out of reach. It was made possible only with the advent of one-atom masers in late 1980s, by Rempe, Walther and Klein [2], to experimentally study the interaction of a single atom and a single resonant mode of electromagnetic field in a cavity. Jaynes-Cummings model (J-C Model) serves to understand the relationship between quantum theory of radiation and semi-classical theory of atom-light interaction. The field of cavity quantum electrodynamics (CQED) was further advanced by putting cold atoms into the high finesse optical cavities [3–5]. Unlike “hot” atoms, cold atoms’ center-of-mass motion (COM) can no longer be neglected in this “atom + cavity” system. One needs to seek a self-consistent solution for both light and atom by treating them on equal footing. Because intra-cavity photon and

atoms very frequently scatter off each other due to the geometric confinement, not only dipole force gets strongly enhanced but also atom's back-action *onto* light becomes significant. For Bose-Einstein condensate (BEC), atoms occupy the same motional quantum state, and because of long-range cavity photon mediation, the internal states (pseudo-spins) are infinitely coordinated. The most famous example is the Dicke model [6], which has been realized in CQED as well [7].

Another recent breakthrough in cold atoms stems from the realization of artificial (synthetic) gauge potentials for neutral atoms, first in bosonic systems [8,9] and later in fermionic counterparts [10,11]. Laser fields are properly aligned and designed in such a way that trapped atoms may mimic charged particles in a magnetic field with emergence of Lorentz-like force. The synthesis is achieved by inducing two-photon Raman transition between two hyperfine ground states. Using a group of degenerate (or quasi-degenerate) pseudo-spin eigenstates, non-abelian dynamics of cold atoms in light fields is generated, which effectively leads to the spin-orbit coupling (SOC) for cold atoms, simulating the electronic counterpart in condensed matter. Here, synthetic SOC refers to the coupling between pseudo-spins (i.e. hyperfine states) and atom's COM motion, rather than the generic interaction between electron's spin (or magnetic moment) and angular/linear momentum operator in quantum mechanics. SOC is essential in understanding numerous underlying condensed matter phenomena and particle physics [12], including *inter alia* topological insulators, Majorana and Weyl fermions, spin-Hall effects, etc [13–17].

In this work, we first briefly review our previous proposal [18], and theoretically explore the full quantum mechanical treatment beyond semi-classical mean field formalism, then investigate the correspondences in quantum and semi-classical regions. We consider a single atom (or an ensemble of  $\mathcal{N}$  non-interacting bosons) being confined by a single-mode unidirectional ring cavity, whose cavity mode together with an additional coherent laser beam form a pair of Raman beams that flips atomic transition between  $|\uparrow\rangle$  and  $|\downarrow\rangle$  while transferring recoil momentum of  $\pm 2\hbar q_r \hat{z}$  from and/or to photon field. Hence, the so-realized effective coupling between atom's external and internal degrees of freedom is generated by the quantized light field, which is affected by atomic dynamics in return. In this sense, the *cavity-assisted* SOC becomes *dynamic*. We show that, at mean field level, the dynamic SOC dramatically modifies the atomic dispersion relation, in particular, with emergence of a loop structure under certain circumstances. We systematically characterize dispersion relation of atomic state and photon number, both as a function of atom's quasi-momentum. For given cavity parameters, we found with increasing Raman coupling strength  $\Omega$ , dispersion curve changes from double minima to gapped single minimum, looped structure, and gapless single minimum in sequence. Furthermore, we carry out the full quantum mechanical treatment by solving master equations of density operators, and find good agreement by comparing averaged photon number with mean field results in limiting parameter regions. The two distinctively different approaches give us an unified understanding of the atom-light effective non-linearity and induced dynamical instability in this system. **how do we cite papers by David Feder, Hui Zhai, Su Yi, etc in this paragraph?**

The article is organized as the following: After briefly reviewing key ideas of our previous work and semi-classical mean field approach in Sec. 2, we develop the full quantum mechanical formalism to the physical system of interest in Sec. 3 and discuss about the intimate correspondence between the two in Sec. 4, and finally conclude in Sec. 5.

## 2. Model Setup and Semi-classical Mean Field Formalism

We follow the effective model Hamiltonian proposed in [18],

$$\begin{aligned} \mathcal{H}_{\text{eff}} = & \sum_{\sigma} \int d\mathbf{r} \left[ \psi_{\sigma}^{\dagger}(\mathbf{r}) \left( \frac{\mathbf{k}^2 + 2\alpha q_r k_z}{2m} + \alpha\delta \right) \psi_{\sigma}(\mathbf{r}) \right] + \frac{\Omega}{2} \int d\mathbf{r} \left[ \psi_{\uparrow}^{\dagger}(\mathbf{r}) \psi_{\downarrow}(\mathbf{r}) c + h.c. \right] \\ & + i\varepsilon_p(c^{\dagger} - c) - \delta_c c^{\dagger} c - i\kappa c^{\dagger} c, \end{aligned} \quad (1)$$

where  $\psi_{\sigma}(\mathbf{r})$  ( $\sigma = \uparrow, \downarrow$ ) is the atomic operator after gauge transformation in rotating frame at pump frequency  $\omega_p$ .  $\alpha = \pm 1$  for  $\sigma = \uparrow, \downarrow$ , respectively.  $q_r$  denotes recoil momentum,  $\delta$  represents the two-photon Raman detuning,  $\varepsilon_p$  refers to pumping rate, and  $\delta_c$  is the cavity-pump detuning.  $\Omega$  describes the atom-photon coupling strength, however, the entire Raman coupling term  $\frac{\Omega}{2} \int d\mathbf{r} e^{+2iq_r z} \Psi_{\uparrow}^{\dagger}(\mathbf{r}) \Psi_{\downarrow}(\mathbf{r}) c e^{+i\omega_R t}$  together with its hermitian conjugate describe cavity-assisted two-photon Raman transition processes, where cavity photon amplitude of  $c$  or  $c^{\dagger}$  is explicitly taken into consideration. It is this coupling that renders the resulting SOC *dynamic*. Furthermore, in the semi-classical approach, we have treated the leakage of cavity photon phenomenologically by introducing a cavity decay rate  $\kappa$ .

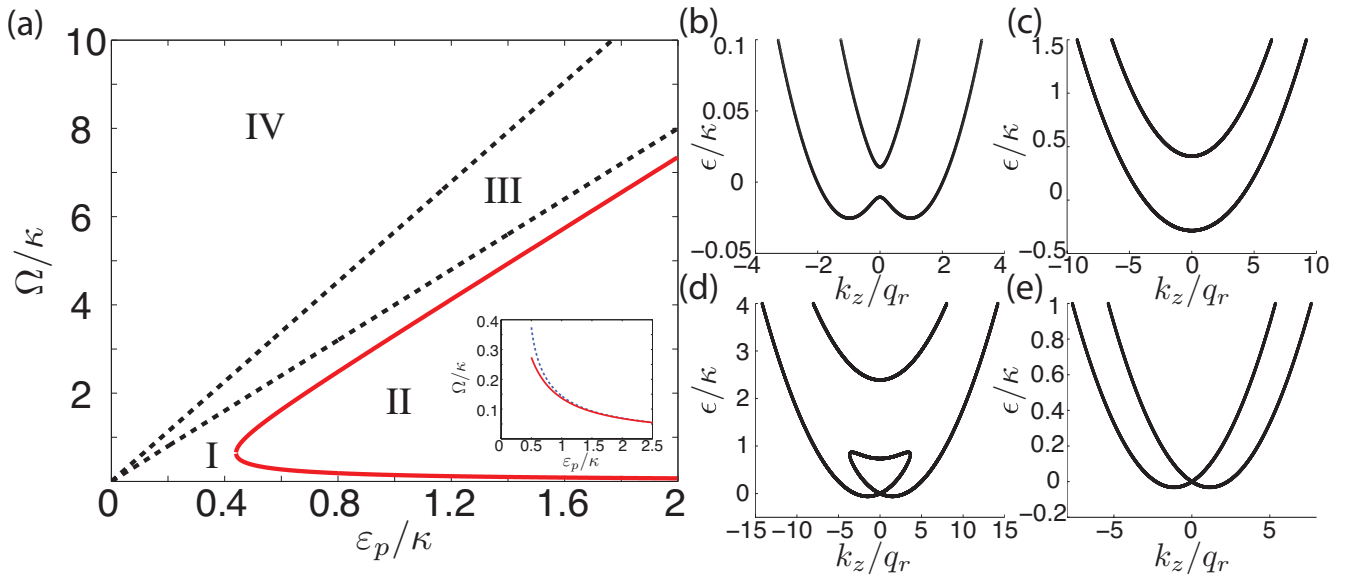


**Figure 1.** Single particle eigen-energy spectrum “phase diagram”. For given parameter  $\delta_c = \kappa$  and  $\delta = 0$ , the behavior of dispersion is divided into four categories which are represented by in (a) from I to IV. From (b) to (e), we fix  $\varepsilon_p = \kappa$ . In region I, the dispersion has double minima as shown in (b) with  $\Omega = 0.03\kappa$ ; region II is enclosed by the red solid curve in (a) and we show the typical point in (c) ( $\Omega = \kappa$ ) where only single minimum exists in the lower helicity band; region III is represented by the black dashed lines in (a) and it is a region where loop structure emerge, as in (d) with  $\Omega = 5\kappa$ ; finally, in region IV we recover the double minimum dispersion although it’s different from region I by closing the gap at  $k_z = 0$ , as in (e) with  $\Omega = 8\kappa$ . In the inset it shows a comparison between the region I boundary (red curve) and large pumping rate limit of classical result given by the function  $4E_r \frac{\sqrt{\kappa^2 + \delta_c^2}}{\varepsilon_p}$ .

From the Hamiltonian (1), one can easily obtain the EOM in Heisenberg picture. To make progress, we adopt the mean-field approximation by replacing the operators by their respective expectation values:

74  $c \rightarrow \langle c \rangle$ ,  $\psi_\sigma(\mathbf{r}) \rightarrow \langle \psi_\sigma(\mathbf{r}) \rangle \equiv \varphi_\sigma(\mathbf{r})$ . Assuming spatial homogeneity, we further take the plane-wave  
 75 ansatz for the atomic modes  $\varphi_\sigma(\mathbf{r}) = e^{i\mathbf{k}\cdot\mathbf{r}}\varphi_\sigma$  with the normalization condition  $|\varphi_\uparrow|^2 + |\varphi_\downarrow|^2 = \mathcal{N}$ . The  
 76 steady-state solution for the photon field is obtained by taking the time derivative of the photon field to  
 77 be zero, which is exact by itself without making further approximations. After some algebra, we write  
 78 the coupled nonlinear time-dependent equations for the two spin components as,

$$i\dot{\varphi}_\uparrow = \left( \frac{\mathbf{k}^2}{2m} + q_r k_z + \delta \right) \varphi_\uparrow + \frac{\Omega \varepsilon_p - i\frac{\Omega}{2}\mathcal{N}\varphi_\downarrow^*\varphi_\uparrow}{2(\kappa - i\delta_c)} \varphi_\downarrow, \quad (2)$$

$$i\dot{\varphi}_\downarrow = \left( \frac{\mathbf{k}^2}{2m} - q_r k_z - \delta \right) \varphi_\downarrow + \frac{\Omega \varepsilon_p + i\frac{\Omega}{2}\mathcal{N}\varphi_\uparrow^*\varphi_\downarrow}{2(\kappa + i\delta_c)} \varphi_\uparrow. \quad (3)$$

79 For a given atomic quasi-momentum  $\mathbf{k}$ , we define eigenstate and eigenenergy as the solution of the  
 80 time-independent version of Eqs. (2) and (3), by replacing  $i(\partial/\partial t)$  with  $\epsilon(\mathbf{k})$ . We consider  $\mathcal{N} = 1$  and  
 81 always take  $k_x = k_y = 0$  hereafter. After some lengthy nonetheless straightforward algebra, we find  
 82 that  $\epsilon(\mathbf{k})$  obeys a quartic equation where detailed derivations are better elaborated in the Supplementary  
 83 Material of [18].

84 We can gain some insights about the general structure of the dispersion relation  $\epsilon(\mathbf{k})$ , e.g. the  
 85 degeneracy condition and the appearance and disappearance of the loop. Simple analysis shows that  
 86 there should be a total of four regimes. (i) As denoted by region I in Fig. 1(a) and (b), we show the  
 87 dispersion curve exhibits a double minima structure. What is different from the degeneracy condition  
 88 given by the synthetic SOC Hamiltonian, is that for arbitrarily small  $\Omega$ , there *always* are double minima  
 89 in the dispersion. (ii) In region II of Fig. 1(a) and (c), the dispersion curve has only single minimum.  
 90 (iii) When  $\Omega_c^{(1)} \equiv 4\varepsilon_p \leq \Omega \leq 4\varepsilon_p\sqrt{1 + (\delta_c/\kappa)^2} \equiv \Omega_c^{(2)}$ , there are total of four real roots allowed by  
 91 the quartic equation — two degenerate roots at  $\epsilon = 0$  and two additional roots with the same sign, see  
 92 for instance Fig. 1(d). Region III corresponds to the region with loop structure and in Fig. 1(a) the two  
 93 dashed black line are numerically obtained by examining the sign of second order derivative of the root  
 94 with respect to  $k_z$ . It also agrees with the analytic expression for  $\Omega_c^{(1)}$  and  $\Omega_c^{(2)}$  as a function of  $\varepsilon_p$ . (iv)  
 95 Finally, when  $\Omega > \Omega_c^{(2)}$ , only the two degenerate roots at  $\epsilon(k_z = 0) = 0$  exist and in Fig. 1(a) and (e) we  
 96 show the double minimum dispersion curve and gapless point at  $k_z = 0$ .

97 We remark that the introduction of cavity photon feedback dramatically alters the dispersion relation,  
 98 where one we could obtain from current proposals concerning synthetic SOC setups. As a matter  
 99 of fact, due to cavity mediation, the emergent loop structure is a distinctive nonlinear feature of the  
 100 system. Furthermore, upon studying the linearized perturbative expansion on top of fixed point solution  
 101 to Eq. 2 and Eq. 3, we have found intriguing dynamical stability properties, where there *always* exist both  
 102 dynamically stable and unstable branches regardless whether there is loop or not [18]. Nonetheless, if we  
 103 consider the large limit of pumping rate  $\varepsilon_p$ , we will again be able to recover synthetic SOC limit. In this  
 104 scenario, cavity photon field becomes the coherent state. One can define the effective Raman coupling  
 105 amplitude  $|\tilde{\Omega}| = \frac{\Omega}{2} \frac{\varepsilon_p}{\sqrt{\kappa^2 + \delta_c^2}}$  and particularly, when  $\Omega < 4E_r \frac{\sqrt{\kappa^2 + \delta_c^2}}{\varepsilon_p}$  dispersion curve has degenerate  
 106 double minimum and when  $\Omega > 4E_r \frac{\sqrt{\kappa^2 + \delta_c^2}}{\varepsilon_p}$  we only have a single minimum in the dispersion curve. As  
 107 we show in the inset of Fig. 1, the numerically determined boundary curve asymptotically approaches the  
 108 black dashed line which is given by the large pumping rate prediction. Note, in large  $\varepsilon_p$  limit, dynamical

instability decay rate  $\gamma$  is also strongly suppressed to a small value, such that the system fully recovers the synthetic SOC Hamiltonian.

As we will also emphasize in Sec. 4, the synthesis of cavity confinement and Raman coupling is not a trivial combination, but rather gives rise to new and subtle physics that deserves more scrutiny. In order to better address the intricate coupling between atom and photon, we dedicate the Sec. 3 and Sec. 4 to explore more on the quantum nature of this system.

### 3. Master Equation Approach: Full Quantum Mechanical Treatment

Semi-classical mean field approach gives an intuitive picture of understanding the atom-light interaction, as we have shown above. However, it ignores quantum fluctuations of both operators  $c$  and  $\psi_\sigma(\mathbf{r})$ . A more stringent approach is given by solving quantum master equation. The quantum master equations, in a nutshell, are differential equations for the density operators, including contributions from off-diagonal elements which represents quantum coherence characteristically. Master equation is generally considered to be more general than the Schrödinger equation, since it uses the density operator instead of a specific state vector and can therefore give statistical as well as quantum mechanical information.

Instead of treating the leakage of cavity photon phenomenologically in Eq. (1), we model the dissipation process by Liouvillian terms  $\mathcal{L}$  appearing in the Lindblad master equation for the atom-field density operator, i.e.,

$$\dot{\rho} = \frac{1}{i\hbar}[H_{\text{eff}}, \rho] + \mathcal{L}\rho. \quad (4)$$

where  $H_{\text{eff}}$  is the same as  $\mathcal{H}_{\text{eff}}$  in Eq. (1) by dropping the last term, i.e.  $-i\kappa c^\dagger c$ . Cavity loss is accommodated by the standard form of Lindblad superoperator [19,20],

$$\mathcal{L}\rho = \kappa(2c\rho c^\dagger - c^\dagger c\rho - \rho c^\dagger c). \quad (5)$$

Again, due to spatial homogeneity, we decouple momentum eigenstates by taking the plane-wave ansatz for the atomic modes as  $\varphi_\sigma(\mathbf{r}) = e^{i\mathbf{k}\cdot\mathbf{r}}\varphi_\sigma$ . Thereon, we are granted to work under the Hilbert subspace of a given momentum value  $\mathbf{k}$ . Here we explicitly write the commutator as,

$$\begin{aligned} [H_{\text{eff}}(\mathbf{k}), \rho] &= \left( \frac{\mathbf{k}^2}{2m} + \frac{q_r k_z}{m} + \delta \right) (\varphi_\uparrow^\dagger \psi_\uparrow \rho - \rho \varphi_\uparrow^\dagger \psi_\uparrow) + \left( \frac{\mathbf{k}^2}{2m} - \frac{q_r k_z}{m} - \delta \right) (\psi_\downarrow^\dagger \varphi_\downarrow \rho - \rho \varphi_\downarrow^\dagger \psi_\downarrow) \\ &+ \mathcal{N} \frac{\Omega}{2} (\varphi_\uparrow^\dagger \varphi_\downarrow c \rho + c^\dagger \varphi_\downarrow^\dagger \varphi_\uparrow \rho - \rho \varphi_\uparrow^\dagger \varphi_\downarrow c - \rho c^\dagger \varphi_\downarrow^\dagger \varphi_\uparrow) \\ &+ i\varepsilon_p (c^\dagger \rho - c\rho - \rho c^\dagger + \rho c) - \delta_c (c^\dagger c\rho - \rho c^\dagger c). \end{aligned} \quad (6)$$

To solve the operator equation, Eq. 4, we choose our basis state as direct product state  $|n; \sigma\rangle$ , where  $n$  denotes non-negative integer photon number and atomic pseudo-spin state is represented by  $\sigma = \uparrow, \downarrow$ . Our goal is to calculate the entire matrix elements of density operator under this set of basis states, denoted

by  $\langle m; \sigma | \rho | n; \sigma' \rangle \equiv \rho_{mn}^{\sigma\sigma'}$ . Without loss of generality, we have taken atom number  $\mathcal{N} = 1$  to simply discussions. We found the governing EOM can be written as,

$$\begin{aligned} \frac{d}{dt} \rho_{mn}^{\sigma\sigma'} &= -i \left( \frac{\mathbf{k}^2}{2m} + \frac{q_r k_z}{m} + \delta \right) (\delta_{\sigma\uparrow} - \delta_{\sigma'\uparrow}) \rho_{mn}^{\sigma\sigma'} - i \left( \frac{\mathbf{k}^2}{2m} - \frac{q_r k_z}{m} - \delta \right) (\delta_{\sigma\downarrow} - \delta_{\sigma'\downarrow}) \rho_{mn}^{\sigma\sigma'} \\ &+ \frac{\Omega}{2i} (\delta_{\sigma\uparrow} \sqrt{m+1} \rho_{m+1n}^{\bar{\sigma}\sigma'} + \delta_{\sigma\downarrow} \sqrt{m} \rho_{m-1n}^{\bar{\sigma}\sigma'} - \delta_{\sigma'\uparrow} \sqrt{n+1} \rho_{mn+1}^{\sigma\bar{\sigma}'} - \delta_{\sigma'\downarrow} \sqrt{n} \rho_{mn-1}^{\sigma\bar{\sigma}'}) \\ &+ \varepsilon_p \left( \sqrt{m} \rho_{m-1n}^{\sigma\sigma'} - \sqrt{m+1} \rho_{m+1n}^{\sigma\sigma'} + \sqrt{n} \rho_{mn-1}^{\sigma\sigma'} - \sqrt{n+1} \rho_{mn+1}^{\sigma\sigma'} \right) \\ &+ i\delta_c (m-n) \rho_{mn}^{\sigma\sigma'} + \kappa \left( 2\sqrt{m+1} \sqrt{n+1} \rho_{m+1n+1}^{\sigma\sigma'} - (m+n) \rho_{mn}^{\sigma\sigma'} \right), \end{aligned} \quad (7)$$

where  $\bar{\sigma}$  represents the flip-spin value, i.e.  $\bar{\uparrow} = \downarrow$  and  $\bar{\downarrow} = \uparrow$ .

With Eq. 7, we can study dynamical evolution of density operator  $\rho$  for a given initial state. For instance, we can initiate the system with a pure state  $|0; \uparrow\rangle$ , construct density operator  $\rho = |0; \uparrow\rangle\langle 0; \uparrow|$ , and let it evolve according to Eq. 7 until all components reach their respective steady state. Although at  $t = 0$  we have  $\text{Tr}[\rho^2] = 1$ , at later times, we will always have  $\text{Tr}[\rho^2] < 1$  for nonzero  $\kappa$ , because cavity decay term renders the system into mixed states.

Assuming the fate of time evolution gives the steady state solution, we can also solve the set of equations after equating the RHS of Eq. 7 to zero. Numerically, this is achieved by introducing a large truncation value  $N$  for maximum number of cavity photon under consideration, such that the problem reduces to simple linear algebra manipulations. In the following, we mainly focus on the steady-state solution of density operator and ignore the transient dynamics.

In order to further quantitatively characterize atom-photon interaction in this open system, we invoke the easily computable entanglement measure for mixed-state, the so-called negativity [21], defined as  $\mathcal{N}(\rho) = \frac{\|\rho^{TA}\|_1 - 1}{2}$ , where  $\|\rho^{TA}\|_1$  denotes the trace norm of partial transpose of density operator with respect to atom party (the same is true for photon party). Density matrix  $\rho$  itself gives all positive definite eigenvalues and thus the trace norm  $\|\rho\|_1 = \text{Tr}[\sqrt{\rho^\dagger \rho}] = \text{Tr}[\rho] = 1$ . Although the partial transpose  $\rho^{TA}$  still satisfies  $\text{Tr}[\rho^{TA}] = 1$ , it does not necessarily guarantee positive definiteness in eigenvalues. The trace norm is written generally as  $\|\rho^{TA}\|_1 = 1 + 2 \sum_i |\mu_i|$  where we have denoted negative eigenvalues as  $\mu_i < 0$ . Thus, by definition, the negativity  $\mathcal{N}(\rho)$  is equal to  $\sum_i |\mu_i|$ , which measures by how much  $\rho^{TA}$  fails to be positive definite. An immediate consequence for any separable (unentangled) state  $\rho_s$  is that  $\mathcal{N}(\rho_s) = 0$ , while for unseparable mixed state,  $\mathcal{N}(\rho)$  is believed to be a good entanglement measure.

## 4. Results and Discussions

With above preparations, we are now in a position to discuss about the results given by the two approaches, and address their relationship. As we have shown above and also in previous work [18], the cavity feedback dramatically modifies single particle dispersion relation. For instance, in intermediate region of atom-photon coupling strength of  $\Omega$ , a loop structure emerge from the center tip of the eigenenergy spectrum. Additionally, in this effective nonlinear system, although atom-photon coupling is linear, dispersion spectrum possesses intriguing stability/instability properties. What we have shown in [18] also indicates that only part of the dispersion is stable for a given quasi-momentum state  $\mathbf{k}$ . The instability analysis prescribes a recipe to map out regions whether fluctuations around fixed point



162 solution would grow exponentially or not. Tout de suite, we apply the formalism developed in Sec. 2  
 163 and Sec. 3 to calculate photon number expectation value inside the cavity.

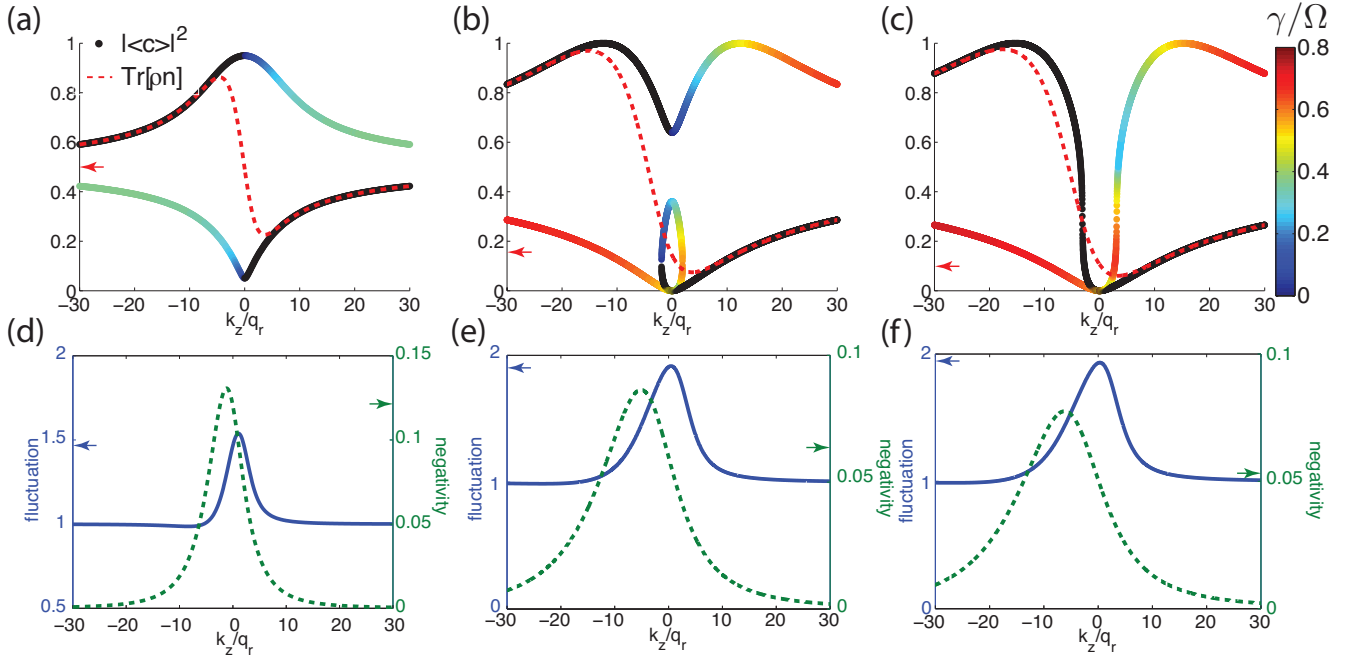


**Figure 2.** Photon number comparison between semi-classical mean field result and full quantum mechanical master equation solution. From (a) to (c),  $\Omega = 3\kappa, 5.6\kappa, 6\kappa$  and colorbar represents the renormalized decay rate  $\gamma/\Omega$  of unstable states and red dashed lines are master equation solutions. Figures from (d) to (f) show the corresponding photon number fluctuation (blue solid curve) and negativity (green dashed line). Other parameters are  $\varepsilon_p = \kappa, \delta_c = \kappa, \delta = 0$  and  $\kappa = 1$  in the dimensionless unit. Although we have chosen  $q_r = 0.22$  in our units (based on a realistic experimental parameter estimate) throughout all figures, we use arrows on vertical axis to denote results concerning  $q_r = 0$  limit.

164 As we show in Fig. 2(a)-(c), we plot semi-classical mean field photon number  $|\langle c \rangle|^2$  and quantum  
 165 mechanical master equation result  $\text{Tr}[\rho n]$ , against atom's dimensionless quasi-momentum  $k_z/q_r$ . From  
 166 semi-classical mean field result, with increasing magnitude of  $\Omega$ , we sweep over regions with only two  
 167 real roots, four real roots and only one double root (at  $\epsilon = 0$ ) to the mean field solution of the quartic  
 168 equation. We can further perform dynamical analysis [18] to pinpoint stable (black dots) and unstable  
 169 branches of the semi-classical solution. For unstable states, we use colorbar to denote the renormalized  
 170 decay rate  $\gamma/\Omega$  where  $\gamma$  refers to the largest real eigenvalue of perturbed dynamical equation [18]. For  
 171 comparison, with the same parameter set, we start from quantum master equation Eq. 7, obtain steady  
 172 state solution of density operator, and trace over the product of density operator and photon number, i.e.  
 173  $\langle n \rangle = \text{Tr}[\rho n]$ . Unlike semi-classical mean field theory, we can only have one unique solution of steady  
 174 state density operator, thus only one branch of average photon number is found as a function of  $k_z$ , as  
 175 represented by the red dashed line in Fig. 2(a)-(c).

176 We found, remarkably, that  $\text{Tr}[\rho n]$  asymptotically approaches  $|\langle c \rangle|^2$  value in dynamically stable  
 177 branches at large  $|k_z|$  limit. This agreement, first of all, further validates our previous dynamical  
 178 stability analysis of semi-classical mean field theory [18]. Due to momentum exchange of  $\pm 2\hbar q_r \hat{z}$

in the Raman process, atomic states with small quasi-momentum  $|k_z|$  are more coupled with photon field, in comparison to the states with large  $|k_z|$ . One would have naively thought cavity-assisted SOC should naturally provide more coupling between atom and photon field than the system with synthetic SOC, because atomic pseudo-spin state and COM are both coupled to cavity photon here. However, it is the SOC that renders this coupling *depends* on atomic quasi-momentum: (i) Momentum exchange plays a major role at small  $k_z$  where two SOC bands are avoided-crossing, and eigenstate is a strong hybridization between bare atomic pseudo-spin states. Thus atom and photon is strongly coupled in this region. (ii) While at large  $k_z$  limit, energy separation becomes so large that the two dressed states are more like two independent bare atomic pseudo-spin states  $|\uparrow\rangle$  and  $|\downarrow\rangle$ . Atomic spin state, COM and photon field are all decoupled in this limit.

Second, the relationship between semi-classical mean field theory and quantum master equation approach can be complementarily understood from photon number fluctuation, which by definition is given by  $\frac{\langle(\Delta n)^2\rangle}{\langle n\rangle} = \frac{\langle n^2\rangle - \langle n\rangle^2}{\langle n\rangle}$ . In Fig. 2(d)-(f), on the left  $y$ -axis, we plot the renormalized fluctuation magnitude as a function of  $k_z$ , shown as blue solid curve. We found it degrades to one in large  $|k_z|$  limit, and this is the limit where photon statistics is best modeled by the coherent state (Poissonian statistics) and atom's back-action *onto* photon becomes negligibly small. For small  $|k_z|$  values, the majority part of fluctuation is larger than one, which implies a super-Poissonian photon number distribution, where cavity photon behaves more thermal like. If we have a positive definite probability distribution for photon number, by the application of Cauchy-Schwarz inequality, the fluctuation value would always have to be greater or equal to one. However, there are regions where renormalized fluctuation is smaller than one, e.g. in Fig. 2(d) at small negative  $k_z$  value,  $\frac{\langle(\Delta n)^2\rangle}{\langle n\rangle} \sim 0.95$ , which implies sub-Poissonian photon number distribution as a signature of system being genuinely non-classical.

Third, the degree of entanglement for a mixed-state can be quantitatively characterized by the negativity  $\mathcal{N}(\rho)$  [21], which we briefly mentioned in Sec. 3. In Fig. 2(d)-(f), on the right  $y$ -axis, we plot the negativity against  $k_z/q_r$  for different  $\Omega$  values using green dashed lines. We can see that when photon field approaches its coherent state at large  $|k_z|$ , negativity becomes very close to zero which means the “atom + photon” system becomes separable. When photon fluctuation deviates from one, negativity shows up a pronounced peak in a qualitatively similar manner.

Above observations conclude our discussion on the relationship between semi-classical theory and quantum mechanical master equation approach in the proposed cavity-assisted SOC system. Alternatively, we can also comment on the relationship between cold atom cavity QED physics and the current work. Conventionally, J-C Model is used to describe interaction between a two level atomic state and photon field by ignoring the rest degrees of freedom. In lieu of mimicking J-C Model, we set  $q_r$  to zero in the Hamiltonian and repeat the steady state solution to Eq. 4. Under this setting, atom's kinetic energy only contribute to a dynamical phase that does not affect expectation value of observable, e.g. photon number, fluctuation, etc. Then we choose an arbitrary value of  $k_z$  or ignore  $k_z^2/2m$  term altogether, and compute  $\text{Tr}[\rho n]$ ,  $\frac{\langle(\Delta n)^2\rangle}{\langle n\rangle}$  and  $\mathcal{N}(\rho)$  where we use arrows on the  $y$ -axis to denote their values in Fig. 2. As we can observe in Fig. 2 from (a) to (c), photon number in J-C Model limit is very different from the one by considering cavity-assisted SOC, *even* in large  $k_z$  asymptotic limit. We have  $\text{Tr}[\rho n] \approx 0.49, 0.14, 0.11$  from (a) to (c), while we always have asymptotic value of  $\frac{\varepsilon_p^2}{\kappa^2 + \delta_c^2}$  independent of  $\Omega$  value in our system, which is 0.5 in Fig. 2. However, we are able to recover J-C model by



simultaneously setting both  $q_r$  and  $\Omega$  to zero, where there is only generic atomic spin and photon coupling present. In Fig. 2 from (d) to (f), we have  $\frac{\langle(\Delta n)^2\rangle}{\langle n\rangle} \approx 1.47, 1.91, 1.93$  and  $\mathcal{N}(\rho) \approx 0.12, 0.06, 0.05$ , respectively.

## 5. Conclusion and Outlook

In this work, we have studied spin-orbit coupled cold atoms inside a ring cavity system, employing both semi-classical mean field theory and full quantum mechanical master equation approach. By treating both light and atom on equal footing and seeking the self-consistent solution in both approaches, we have found cavity-assisted SOC dramatically modified atomic dispersion relation, intriguing dynamical instabilities, and atom's back-action onto light field also leads to non-trivial atom-photon coupling that are fundamentally different to the system with either synthetic SOC or J-C model type of interaction. We have also explored correspondence and discussed the relationship between the two approaches. We conclude that the synthesis of cavity QED and SOC is not a trivial combination and interesting new physics are emergent in this setting. The two distinctively different approaches give us an unified understanding of the atom-light effective non-linearity and induced dynamical instability in this system.

Although for simplicity reasons we have only considered one atom inside the cavity, the current formalism and results can be easily generalized to  $\mathcal{N}$  identical non-interacting bosons, where we would expect similar physics involving atom and light couplings. However, due to anti-symmetrization constraint, for  $\mathcal{N}$  non-interacting fermions, it is less straightforward to bridge a connection. Furthermore, it would be interesting to consider atom-atom interactions for the many body case [cite Feder's paper here?](#) and study super-radiant Dicke phase transition [cite Hui Zhai's paper and Xiong-Jun Liu's super-radiant paper here?](#), using the master equation approach.

## Acknowledgments

We acknowledge discussions with Zhengwei Zhou and XXX. H.P. is supported by the NSF and Welch Foundation (Grant No. C-1669 XXX);

## Author Contributions

H.P. conceived the idea of the project, L.D. and C. Z. explored the theoretical and numerical aspects of the physics. All authors contributed to writing and revising the manuscript and participated in the discussions about this work.

## Conflicts of Interest

The authors declare no conflict of interest.

## References

1. E.T. Jaynes, F.W. Cummings (1963). Proc. IEEE 51 (1): 89–109.
2. G. Rempe, H. Walther, and N. Klein (1987). Phys. Rev. Lett. 58 (4): 353–356.

3. Brennecke, F., Donner, T., Ritter, S., Bourdel, T., Kohl, M., and Esslinger, T., *Nature* **2007**, 450 268.
4. Colombe, Y., Steinmetz, T., Dubois, G., Linke, F., Hunger, D. and Reichel, J. *Nature* **2007**, 450 272.
5. Slama, S., Bux, S., Krenz, G., Zimmermann, C. and Courteille, Ph. W. *Phys. Rev. Lett.* **2007**, 98 053603.
6. Dicke, R. H. Coherence in spontaneous radiation processes. *Phys. Rev.* 93, 99–110 (1954).
7. Kristian Baumann, Christine Guerlin, Ferdinand Brennecke Tilman Esslinger. *Nature* 464, 1301–1306 (29 April 2010)
8. Y.-J. Lin, K. Jimenez-Garcia, and I. B. Spielman, *Nature* (London) **2011**, 471, 83.
9. Y.-J. Lin, R. L. Compton, K. Jimenez-Garcia, W. D. Phillips, J. V. Porto, and I. B. Spielman, *Nat. Phys.* **2011**, 7, 531.
10. P. Wang, Z.-Q. Yu, Z. Fu, J. Miao, L. Huang, S. Chai, H. Zhai, and J. Zhang, *Phys. Rev. Lett.* **2012**, 109, 095301.
11. L. W. Cheuk, A. T. Sommer, Z. Hadzibabic, T. Yefsah, W. S. Bakr, and M. W. Zwierlein, *Phys. Rev. Lett.* **2012**, 109, 095302.
12. V Galitski, IB Spielman, *Nature* **2013**, 494 7435.
13. Hasan, M. Z., Kane, C. L. *Rev. Mod. Phys.* **2010**, 82 3045–3067.
14. Sau, J. D., Lutchyn, R. M., Tewari, S. and Sarma, Das, S. *Phys. Rev. Lett.* **2010**, 104 040502.
15. Burkov, A. A. and Balents, L., *Phys. Rev. Lett.* **2011**, 107 127205.
16. Sinova, J., Cilcer, D., Niu, Q., Sinitsyn, N., Jungwirth, T., and MacDonald, A., *Phys. Rev. Lett.* **2004**, 92 126603.
17. Kato, Y. K., Myers, R. C., Gossard, A. C. and Awschalom, D. D., *Science* **2004**, 306 1910–1913.
18. Lin Dong, Lu Zhou, Biao Wu, B. Ramachandhran, and Han Pu, *Phys. Rev. A* **2014** 89, 011602(R).
19. Kossakowski, A. *Rep. Math. Phys.* **1972**, 3 (4): 247.
20. Lindblad, G. *Commun. Math. Phys.* **1976**, 48 (2): 119.
21. Vidal, G., Werner, R. F., *Phys. Rev. A* **2002**, 65 032314.

© March 3, 2015 by the authors; submitted to *Atoms* for possible open access publication under the terms and conditions of the Creative Commons Attribution license <http://creativecommons.org/licenses/by/4.0/>.